

Development of a lower limb rehabilitation exoskeleton based on real-time gait detection and gait tracking

Chao Zhang¹, Gangfeng Liu¹, Changle Li¹, Jie Zhao¹, Hongying Yu² and Yanhe Zhu¹

Abstract

Hemiplegia, apoplexia, or traffic accidents often lead to unilateral lower limb movement disorders. Traditional lower limb rehabilitation equipments usually execute walk training based on fixed gait trajectory; however, this type is unsuitable for unilateral lower limb disorders because they still have athletic ability and initiative walking intention on the healthy side. This article describes a wearable lower limb rehabilitation exoskeleton with a walk-assisting platform for safety and anti-gravity support. The exoskeleton detects and tracks the motion of the healthy leg, which is then used as the control input of the dyskinetic leg with half a gate-cycle delay. The patient can undergo walk training on his own intention, including individual walking habit, stride length, and stride frequency, which likely contribute to the training initiative. The series elastic actuator is chosen for the exoskeleton because the torque output can be accurately detected and used to calculate the assisted torque on the dyskinetic leg. This parameter corresponds to the recovery level of a patient's muscle force. Finally, the walk-assisting experiments reveal that the rehabilitation exoskeleton in this article can provide the necessary assisting torques on the dyskinetic leg, which can be accurately monitored in real time to evaluate a patient's rehabilitation status.

Keywords

Rehabilitation exoskeleton, initiative walk training, real-time gait detection

Date received: 29 July 2015; accepted: 15 December 2015

Academic Editor: Yong Chen

Introduction

Human walking is the most basic mode of coordinated and voluntary movement with smooth transition, appropriate step length, and stable energy consumption.¹ Exercise therapy based on neurodevelopment facilitation theory is a fundamental rehabilitation method for lower limb movement disorders caused by hemiplegia, apoplexia, or accidental disability resulting from traffic accidents or natural disasters.² The application of rehabilitation exoskeletons can free physiotherapists from heavy manual labor and improve

training efficiency in terms of the precise motion control and real-time recording of training parameters; this

¹State Key Laboratory of Robotics and System, Harbin Institute of Technology, Harbin, China

²School of Mechatronics Engineering, Harbin Institute of Technology, Harbin, China

Corresponding author:

Yanhe Zhu, State Key Laboratory of Robotics and System, Harbin Institute of Technology, Harbin 150001, China.

Email: yhzhu@hit.edu.cn



application contributes to the evaluation of rehabilitation. Rehabilitation exoskeletons can be broadly categorized into two types: lower limb wearable style and foot pedal style.

With the exoskeletons of the first type, patients usually undergo training on a treadmill; during training, both legs are tied to the exoskeleton and the upper body is supported by anti-gravity bundling belts. A suspension device is applied to balance the weight of the exoskeleton and part of the patient's body weight. The exoskeletons of this style generally comprise a walk-assisting platform, an exoskeleton of the upper body, and two legs. Foot parts are usually not considered in these exoskeletons, such as WalkTrainer³ and Lokomat⁴ developed in Switzerland, SUBAR developed at Sogang University,⁵ ALEX developed at the University of Delaware,⁶ and lower limb walking assistant robot developed at Zhejiang University.⁷

For the second type, a pair of multi-variant pedal structures is connected to a patient's feet for the rehabilitation training. The advantage of this approach is that uneven ground and changing terrains can be simulated to achieve training diversity. The Skywalker by MIT,⁸ the 6-degree-of-freedom (DOF) gait rehabilitation robot by Sogang University,⁹ and the Haptic Walker by Benjamin Franklin University¹⁰ are significant examples of the second type of exoskeletons.

Traditional lower limb rehabilitation equipments usually execute walk training by driving the legs on the basis of the fixed gait trajectory, which precludes a patient's initiative. As such, they seem unsuitable for unilateral lower limb disorders because the equipment may interfere between the fixed gait trajectory and the initiative walking intention of the healthy leg.

This article proposes a wearable lower limb exoskeleton for the rehabilitation training of unilateral lower limb disorders. A wearable exoskeleton with a walk-assisting device has been designed to help during walk training. The exoskeleton detects and tracks the healthy leg's motion in real time; the exoskeleton also provides the necessary assisting torque of the dyskinetic leg. The main design goals of this article are as follows: to improve the training initiative and to dynamically calculate the muscle torques on the dyskinetic leg, and these torques can be used as an evaluation index of rehabilitation training.

Motion analysis of human lower limbs

The motion analysis of lower limbs is of great significance for the walking mechanisms research and the exoskeleton design. It mainly includes the gait characteristics and its influencing factors. The clinical gait analysis (CGA) data are generally used for the human walking analysis and the exoskeleton design.¹¹ The

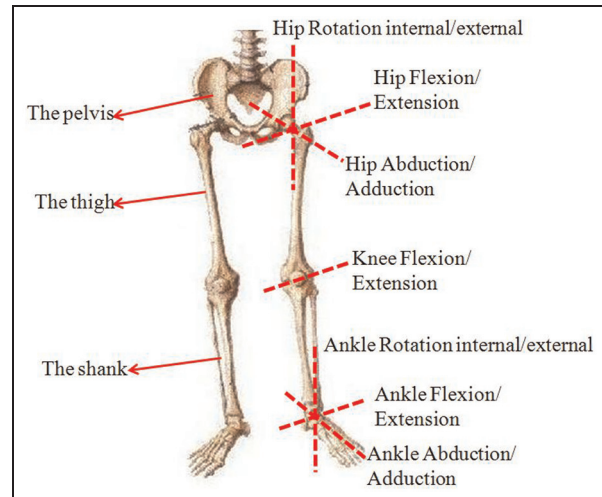


Figure 1. DOFs of human legs.

walking motion is implemented by a multi-dimensional pelvic movement and associated rotations of the hip, knee, and ankle joints. Figure 1 shows the DOFs of the lower limbs. The pelvis plays an important role in maintaining upper balance and increasing the stride length, but its rotation ranges and power consumption are relatively small.¹² So it could be designed as a passive joint. The movements with relatively large rotation ranges are the flexion/extension rotation at the hip, knee, and ankle joints. And the rotation ranges are about 50°, 60°, and 20° in sequence. The other DOFs at the hip and ankle joints are also with micro motions to perform a harmonious and natural walking posture. This will contribute to the vertical upper body and ensure the center of gravity is located between the two feet. As there is a walk-assisting device to keep balanced walking and to support the exoskeleton weight and part of the patient's body weight, the foot parts tend to be not necessary. Finally, the designing architecture is determined as active driving at hip and knee, and passive rotation joints for the pelvic movement.

The gait trajectory exhibits individual differences. In general, individual walking habits, different walking speeds, and various body weights are the main influencing factors. In a study,¹¹ three groups of CGA data have been provided by detecting different groups of subjects. The walking speed is 1.3 m/s and the body weight is 75 kg. The significant differences are shown on the joint angle curves because of the different walking habits of the subjects. In another study,¹³ the effects of different loads (0, 10, 20, and 30 kg) and walking speeds (0.8, 1.3, and 1.7 m/s) have been evaluated; the results reveal large joint angle deviations in the joint angle trajectories. The maximum joint angle variations caused by different individual walking habits, speeds, and loads are shown in Table 1.

Table 1. Maximum joint angle deviation caused by the three gait influencing factors.^{11,13}

| Gait influencing factors | Maximum joint angle deviation | | |
|----------------------------------|-------------------------------|----------|-----------|
| | Hip (°) | Knee (°) | Ankle (°) |
| Individual walking habits | 13 | 18 | 10 |
| Different walking speeds | 8 | 13 | 5 |
| Different feet-supported weights | 10 | 12 | 12 |

The large joint angle deviations imply that the fixed gait trajectory is unsuitable for rehabilitation training, especially for patients who suffer from unilateral lower limb disorders but still exhibit an athletic ability and initiative walking intention on the healthy leg. Therefore, intentional walk training can be conducted to drive the dyskinetic leg by real-time detecting and tracking the motions of the healthy leg.

Exoskeleton mechanical design

Several major aspects, such as similar DOF distribution with the human body, human-machine connection method, and walking stability, should be considered in exoskeleton design and system implementation.

Exoskeleton design with the walk-assisting platform

The rehabilitation exoskeleton includes a pelvis segment and two pseudo-anthropomorphic legs. A walk-assisting platform is also required for safety consideration and anti-gravity support. If necessary, a suitable ankle-foot orthosis can be added to the rehabilitation exoskeleton if a patient suffers from some complications, such as foot drop or strephenopodia caused by long-term underactivity.^{14,15}

Pelvic motion is multi-dimensional with small amplitudes. The hip joint exhibits three rotational DOFs as a spherical pair. The knee joint displays a complex skeletal conformation with two DOFs. The knee external/internal rotation is locked when the joint is completely straight and gradually released during the bending process. This rotation DOF could be combined together with the external/internal rotation of the ankle and then not considered. As a result, the knee joint can be designed with one DOF (flexion/extension). Overall, the DOF distribution of the rehabilitation exoskeleton is designed as follows:

1. Three rotational DOFs at the pelvic and three translational DOFs at the walk-assisting platform;
2. Three DOFs at the hip (equivalent to a spherical pair);
3. One DOF at the knee (simplified as a revolute pair).

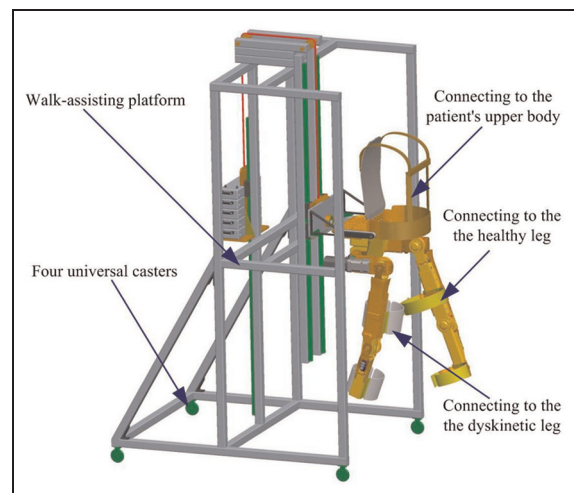


Figure 2. Mobile lower extremity rehabilitation exoskeleton with a walk-assisting platform.

The overall mobile lower extremity rehabilitation exoskeleton is shown in Figure 2. Four universal casters are placed on the walk-assisting platform, and these casters enable the arbitrary direction of walking. The multi-dimensional pelvic motions are also implemented on the walk-assisting platform. As shown in Figure 3(a), the coronal and sagittal axes are determined by two rotational joints. The vertical axis is realized by the motion of four universal casters on the ground. The up-down motion of the human upper body is achieved by a pair of linear guide rails and sliders.

Pseudo-anthropomorphic powered legs mainly function to detect and track the movements of the healthy leg in real time and subsequently to provide necessary torque assistance for the dyskinetic leg. As shown in Figure 3(b), the hip and knee flexion/extension rotations are power driven; the other DOFs passively move along with the human body.

Man-machine connection modes

The functions of the man-machine connections on the healthy and dyskinetic legs are different. On the healthy side, the connection should detect and track the human joint movements in real time. On the dyskinetic side, the connection should provide the necessary assisted torques for the hip and knee joints. Therefore, connection devices should be respectively designed.

The dyskinetic leg should be driven by the exoskeleton; thus, a rigid binding method is applied to the thigh and shank. For the healthy leg, the hip and knee rotations are detected by the 2-DOF flexible bundling device, as shown in Figure 4. The ranges of the two sliding freedoms are both $\pm 10\text{ mm}$ and maintained at the middle position by balance springs. The stiffness coefficient is

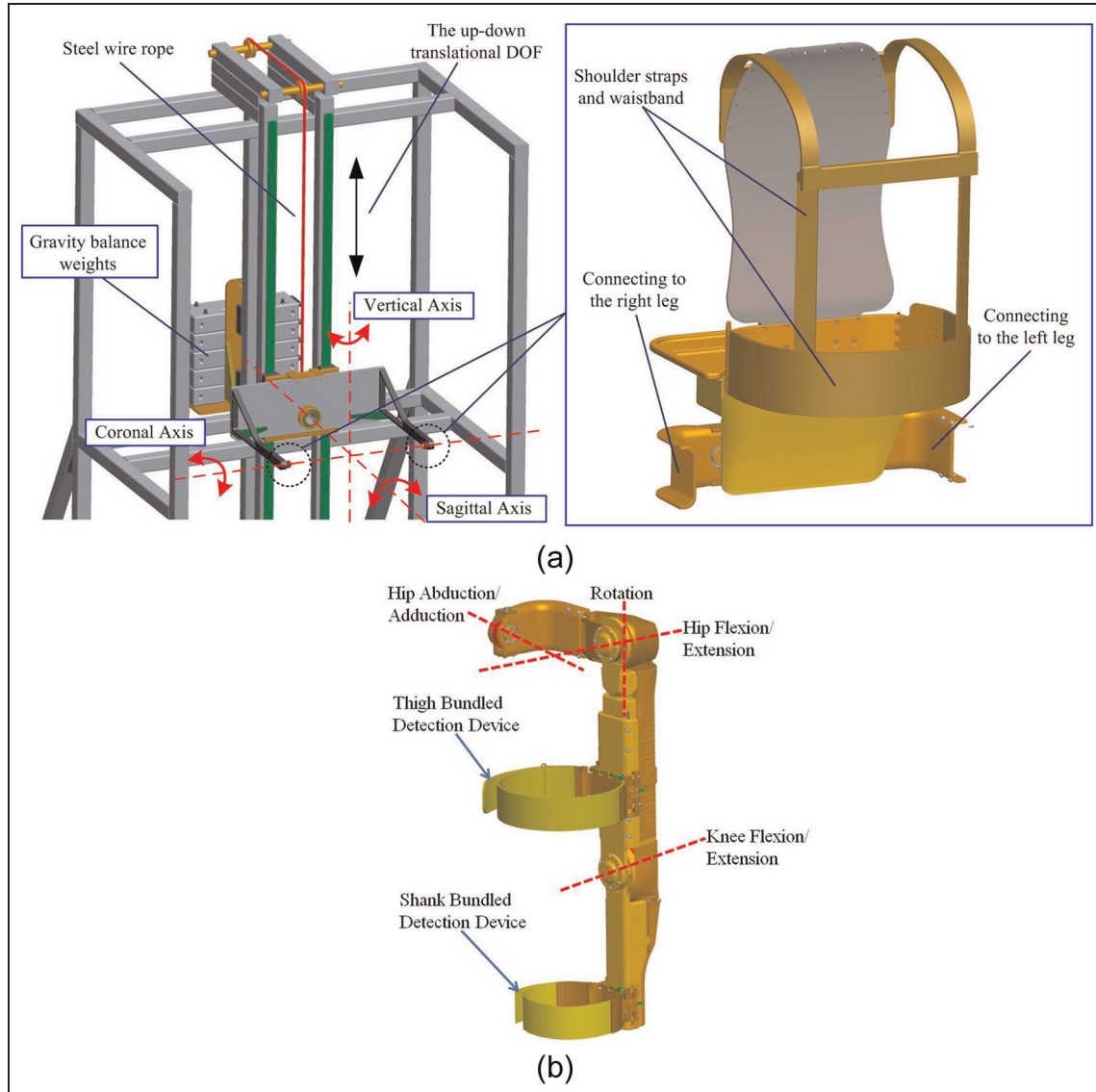


Figure 3. DOFs design of the mobile lower extremity rehabilitation exoskeleton: (a) DOFs design on the walk-assisting platform and (b) DOFs distribution of the exoskeleton leg.

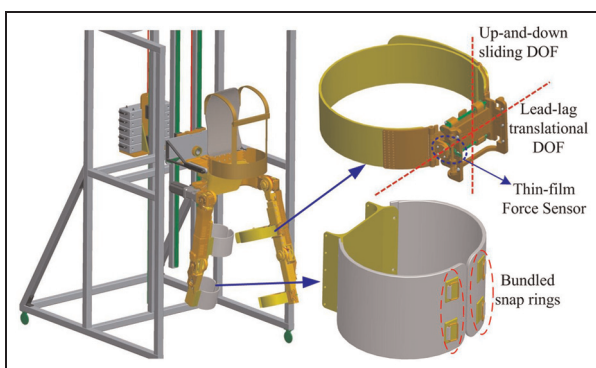


Figure 4. Man-machine connection devices for both the healthy and dyskinetic legs.

very small (2 N/mm) to ensure a relatively low interaction force under the condition of the man-machine position deviation. A thin-film force sensor is placed and preloaded by a pair of balance springs in the lead-lag translational direction. The human movement intentions and the position deviation between the wearer and the exoskeleton are detected by measuring the increase or decrease of the preload force, as shown in Figure 5.

Implementation of the walk-training process

For unilateral lower limb movement disorders, the initiative movement of the healthy leg is used to guide the

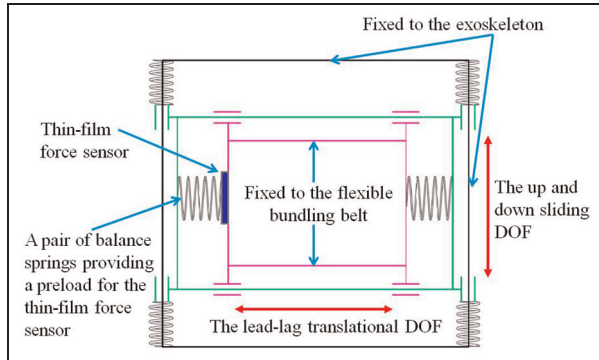


Figure 5. Schematic diagram of the 2-DOF flexible bundling device.

rehabilitation training process. The healthy leg's motion is detected and used as a control input of the dyskinetic leg with half a gate-cycle delay. The exoskeleton tracks the healthy leg and positions the dyskinetic leg on the basis of the detected joint angle trajectories.

Joint angle detection and follow-up control on the healthy leg

On the healthy side, the exoskeleton tracks the joint motions of the human leg in real time and the control goal is to reduce the man-machine interaction forces caused by Δx_1 and Δx_2 to 0 as shown in Figure 6.

The hip rotation centers of the human and the exoskeleton are in a superposition state. The exoskeleton joint angles α_1 and α_2 are detected by angle sensors on the exoskeleton joints. Δx_1 and Δx_2 are the man-machine position deviations. The man-machine interaction forces (F_1 , F_2) are detected by two thin-film force sensors. k is the equivalent stiffness of the balance springs. As a result, the hip and knee angles of the healthy leg can be calculated as follows

$$\theta_1 = \arcsin\left(\frac{F_1}{kd_1}\right) + \alpha_1 \quad (1)$$

$$\theta_2 = \arcsin\left(\frac{h_T F_2 - d_1 F_1}{kd_1 d_2}\right) + \alpha_2 \quad (2)$$

where h_T is the thigh length and d_1 and d_2 are the distances of the bundling belts from the hip and knee joints, respectively.

The block diagram of the follow-up control to the healthy leg is shown in Figure 7. F_{des} is the anticipant interactive force that should be 0; C is the angular transformation as shown in formula (1) and (2); e_θ is the expectation of the joint angle increment; and Θ_H and Θ_E are the angles of human and exoskeleton. A proportional-derivative (PD) controller is used to generate a reference torque, which is then used as the input

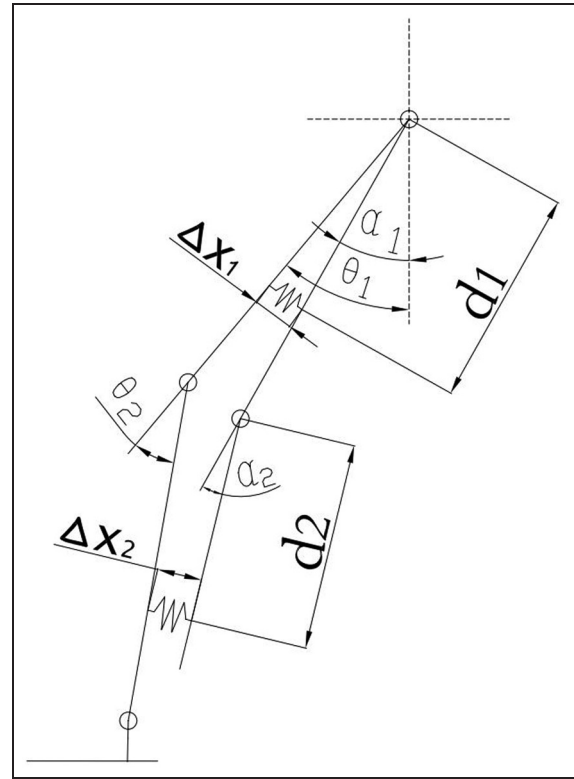


Figure 6. Simplified model of the joint angle detection on the healthy leg.

to the Series Elastic Actuator (SEA) controller. The output torque of SEA is fed to the inner control loop while the man-machine interaction force is fed back to the overall controller. The cycle of the outer control loop is 5 ms. Both the position and torque outputs of the SEA actuator, τ_E and Θ_E , could be detected by sensors.

Position control of the dyskinetic leg

On the dyskinetic side, the calculated hip and knee angles of the healthy leg (θ_1 and θ_2) are used as the control input with half a gate-cycle delay. An active position control method is used as shown in Figure 8, where Θ_{des} is the desired angle, and an outer position control loop is used to ensure that the reference angle is accurately tracked.

Rehabilitation evaluation index

The muscular torque of the dyskinetic leg is the most intuitive evaluation index to evaluate rehabilitation; this value is difficult and inconvenient to detect. A compromise solution is presented by measuring the necessary assisted torques on the dyskinetic leg, and the muscular torque of each patient can be obtained. The SEA is chosen for the exoskeleton joints because the series spring can act as a torque sensor. The structure diagram of the

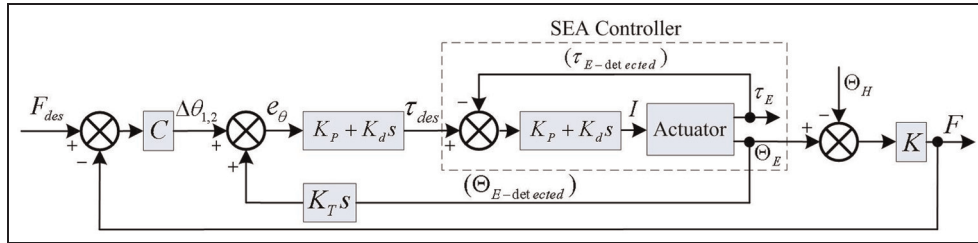


Figure 7. Follow-up control diagram of the healthy leg.

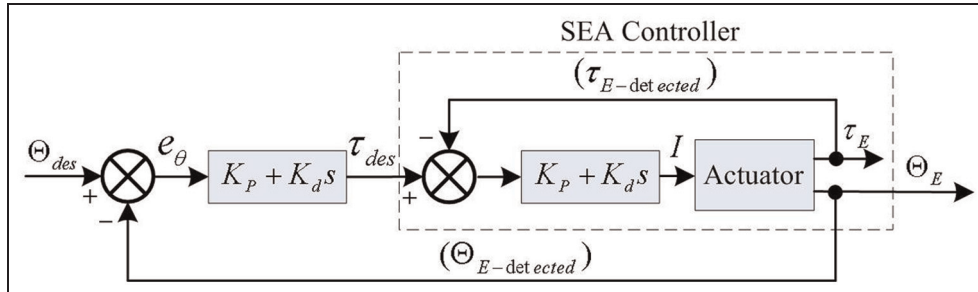


Figure 8. Position control diagram of the dyskinetic leg.

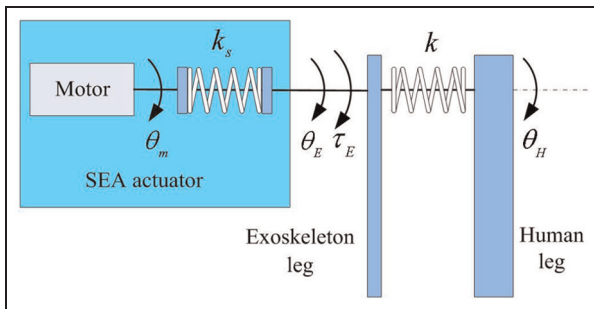


Figure 9. Joint drive model of the exoskeleton.

SEA actuator is presented in Figure 9. The torque output can be accurately obtained as follows

$$\tau_E = k_s \times (\theta_m - \theta_E) \quad (3)$$

where k_s is the stiffness of the series spring and θ_m and θ_E are detected by sensors.

On the healthy side, the motor driving torque (T_{hea}) reflects the consumption of the exoskeleton itself, such as the rotary damper and the inertia. The average value of the human-machine interaction force is approximately 0; as such, the effect of this value is disregarded in this analysis. On the dyskinetic side, the motor driving torque (T_{dys}) includes the assistant torque for the dyskinetic leg (T_a) and the torque consumption by the exoskeleton itself (T_s); $T_s = T_{hea}$. Therefore, the assistant torque for the dyskinetic leg is obtained as follows

$$T_a = T_{dys} - T_{hea} \quad (4)$$

When the dyskinetic leg does not exert any force during walking and its motion is absolutely driven by the exoskeleton, the motor driving torque is T_{total} . As a result, the muscular torque required for normal walking is calculated as follows: $T_{nor} = T_{total} - T_{hea}$. Hence, the dyskinetic leg's muscular torque is expressed as follows

$$T_{mus} = T_{nor} - T_a = (T_{total} - T_{hea}) - (T_{dys} - T_{hea}) = T_{total} - T_{dys} \quad (5)$$

The assistant torque (T_a) and the muscular torque (T_{mus}) on the dyskinetic leg can be used for the rehabilitation evaluation.

Walk-training performance test

Before the test is applied to unilateral lower limb disorder patients, initial walk-assisting experiments should be conducted to evaluate the tracking performance on the healthy leg, the position control performance on the dyskinetic leg, and the walking flexibility.

As shown in Figure 2, the exoskeleton weight is approximately 30 kg. A load of 60 kg is installed on the other side of the walk-assisting platform for gravity balance. The body weight of the subject is approximately 60 kg. So nearly half of the body weight can be supported by the bundling belts on the shoulders and waist to simulate patients with lower limb muscle weakness. Moreover, the gravity balance weight can be increased or decreased to fit different patients. The imitative subject is required to apply minimal exertion on the right leg to simulate the muscle weakness of patients.



Figure 10. Walking process conducted in the laboratory environment.

Table 2. Description of the experiment steps and the data processing.

| Experiment step | Description | Recorded data | Data processing results |
|-----------------|--|---|---|
| 1 | Exoskeleton followed the motion of the human left leg. The exoskeleton joint angles and the man-machine position deviation are detected in real time | 1. Exoskeleton joint angles (α_1, α_2) 2. Motor driving torques ($T_{hea-hip}, T_{hea-knee}$) 3. Force sensors (F_1, F_2) | 1. Joint angles of healthy leg (θ_1, θ_2) |
| 2 | Joint angles of human left leg (θ_1, θ_2) were then used as the control input of the right leg. And the right leg paid slight exertion in this step to detect the assisting torques on the right leg | 1. Motor driving torques of the right leg ($T_{dys-hip}, T_{dys-knee}$) | 1. Assisted torque for the dyskinetic leg (T_a) |
| 3 | Similar to the experiment step 2, the joint angles (θ_1, θ_2) were still used as the control input of the right leg. But the right leg did no exertion and was absolutely driven by the exoskeleton | 1. Motor driving torques of the right leg ($T_{total-hip}, T_{total-knee}$) | 1. Muscular torque required for normal walking (T_{nor}) 2. Dyskinetic leg's own muscular torque (T_{mus}) |

The walking process is shown in Figure 10, and the experimental steps are listed in Table 2.

The exoskeleton is always in the state of weightlessness. On the healthy side, the exoskeleton joint rotations only need to overcome the influence of the inertia, friction, damping, and so on. So the motor driving torques are small. On the dyskinetic side, the exoskeleton needs to drive the dyskinetic leg during the swing phase and then support the body weight during the supporting phase. As a result, the motor driving torques are relatively large.

The interaction forces on the healthy leg are illustrated in Figure 11. The maximum interaction forces on the thigh and shank are less than 10 N. The maximum angle deviations at the hip and knee are calculated as 1.15° and 0.86° , respectively. The small man-machine interaction forces and angle deviations

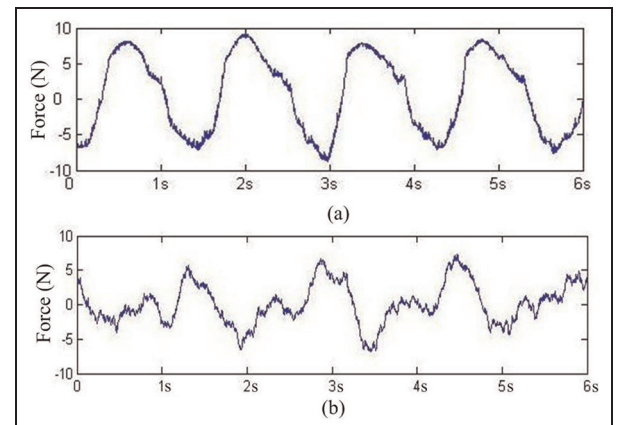


Figure 11. Interaction forces of the healthy leg: (a) the interaction force on the left thigh and (b) the interaction force on the left shank.

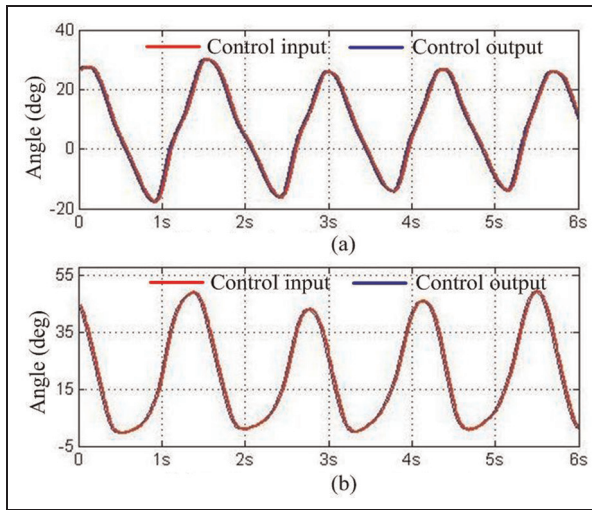


Figure 12. Control input (joint angles of the healthy leg) and the control output (actual angles of the dyskinetic leg): (a) the hip input and output angles and (b) the knee input and output angles.

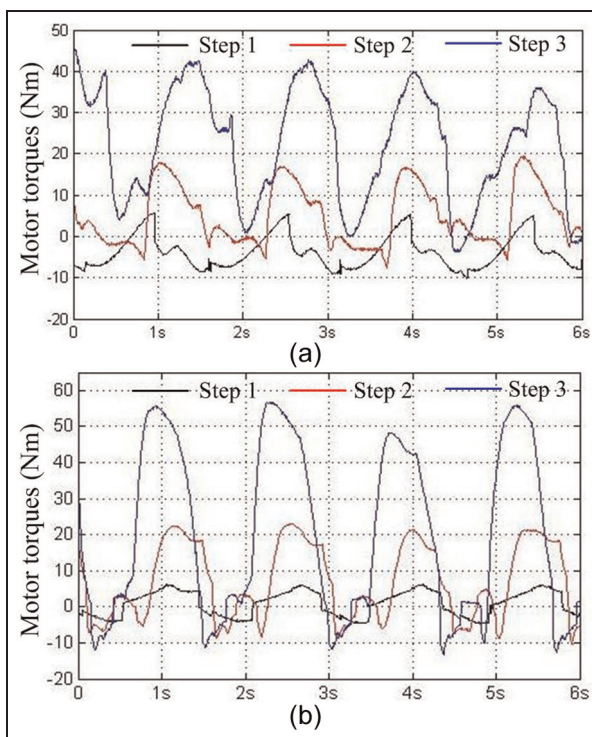


Figure 13. Motor driving torques during the three experimental steps: (a) the motor driving torques at the hip joints and (b) the motor driving torques at the knee joints.

confirm that the exoskeleton can efficiently track the movement of the healthy leg.

For the dyskinetic leg, Figure 12 shows the control input (joint angles of the healthy leg) and the control output

(actual angles of the dyskinetic leg). The two curves are almost coincident, and the transitions are smooth.

The motor driving torques of the three experiment steps were illustrated in Figure 13. The joint torque records during the walk process show that all the muscular torques required for normal walking (T_{nor}), the muscular torque (T_{mus}), and the assisted torque (T_a) on the dyskinetic leg could be obtained dynamically in real time.

Conclusion and future work

A mobile lower limb rehabilitation exoskeleton is presented for the walk training of patients with unilateral leg movement disorders. The mechanical system comprises a lower limb exoskeleton, a walk-assisting platform, and two different styles of man-machine connection devices. The motion of the healthy leg is detected and tracked by the exoskeleton leg, and the recorded motion data are then used as the control input of the dyskinetic leg with half a gate-cycle delay. Initial walking experiments show that the muscular torque (T_{mus}) and the assisted torque (T_a) of the dyskinetic leg can be dynamically detected in real time and used for the rehabilitation evaluation.

Declaration of conflicting interests

The author(s) declared no potential conflicts of interest with respect to the research, authorship, and/or publication of this article.

Funding

The author(s) disclosed receipt of the following financial support for the research, authorship, and/or publication of this article: The work reported in this article is funded by “National High Technology Research and Development Program of China (863 Program)” (Grant No. 2012AA041505) and “Self-Planned Task of State Key Laboratory of Robotics and System (HIT)” (Grant No. SKLRS201201A02).

References

- Zielinska T, Chew CM, Kryczka P, et al. Robot gait synthesis using the scheme of human motions skills development. *Mech Mach Theory* 2009; 44: 541–558.
- Teodorescu HNL and Jain LC. *Intelligent systems and technologies in rehabilitation engineering*. Boca Raton, FL: CRC Press, 2001, pp.3–22.
- Allemand Y, Stauffer Y, Clavel R, et al. Design of a new lower extremity orthosis for overground gait training with the WalkTrainer. In: *Proceedings of the 2009 IEEE 11th international conference on rehabilitation robotics*, Kyoto, Japan, 23–26 June 2009, pp.550–555. New York: IEEE.

4. Jezernik S, Colombo G and Morari M. Automatic gait-pattern adaptation algorithms for rehabilitation with a 4-DOF robotic orthosis. *IEEE T Robotic Autom* 2004; 20: 574–582.
5. Kong K, Tomizuka M and Moon H. Mechanical design and impedance compensation of SUBAR. In: *Proceedings of the 2008 IEEE/ASME international conference on advanced intelligent mechatronics*, Xian, China, 2–5 July 2008, pp.377–382. New York: IEEE.
6. Banala SK, Kim SH, Agrawal SK, et al. Robot assisted gait training with active leg exoskeleton. In: *Proceedings of the second biennial IEEE/RAS-EMBS international conference on biomedical robotics and biomechatronics*, Scottsdale, AZ, 19–22 October 2008, pp.653–658. New York: IEEE.
7. Zhang J, Dong Y, Yang C, et al. 5-Link model based gait trajectory adaption control strategies of the gait rehabilitation exoskeleton for post-stroke patients. *Mechatronics* 2010; 20: 368–376.
8. Artemiadis PK and Krebs HI. Impedance-based control of the MIT-Skywalker. In: *Proceedings of the ASME dynamic systems and control conference*, Cambridge, MA, 12–15 September 2010, pp.389–396. New York: ASME.
9. Kong K and Jeon D. Design and control of an exoskeleton for the elderly and patients. *IEEE/ASME T Mech* 2006; 11: 428–432.
10. Schmidt H, Hesse S, Bernhardt R, et al. HapticWalker—a novel haptic foot device. *ACM Trans Appl Percept* 2005; 2: 166–180.
11. Zoss AB, Kazerooni H and Chu A. Biomechanical design of the Berkeley lower extremity exoskeleton (BLEEX). *IEEE/ASME T Mech* 2006; 11: 128–138.
12. Zhao L, Zhang L and Wang L. Three-dimensional motion of the pelvis during human walking. In: *Proceedings of the IEEE international conference on mechatronics and automation*, Niagara Falls, ON, Canada, 29 July–1 August 2005, pp.335–339. New York: IEEE.
13. Han Y and Wang X. The biomechanical study of lower limb during human walking. *Sci China Technol Sci* 2011; 54: 983–991.
14. Cullell A, Moreno JC, Rocon E, et al. Biologically based design of an actuator system for a knee–ankle–foot orthosis. *Mech Mach Theory* 2009; 44: 860–872.
15. Zhang C, Zhu Y, Fan J, et al. Design of a quasi-passive 3 DOFs ankle-foot wearable rehabilitation orthosis. *Bio-Med Mater Eng* 2015; 26: S647–S654.